Influence of structural inhomogeneity on the luminescence properties of silicon nanocrystallites

I. V. Blonskiĭ,* M. S. Brodyn, A. Yu. Vakhnin, A. Ya. Zhugayevych, V. M. Kadan, and A. K. Kadashchuk

Institute of Physics, National Academy of Sciences of Ukraine, pr. Nauki 46, 03650 Kiev, Ukraine
(Submitted January 10, 2002)
Fiz. Nizk. Temp. **28**, 978–987 (August–September 2002)

The features of the photoluminescence and the manifestation of thermally stimulated and tunneling luminescence due to the separation of nonequilibrium charge carriers between the photoexcited silicon core of a nanocrystallite and its peripheral layers of SiO_x and SiO_2 are investigated for different forms of nanostructured silicon. A model is proposed wherein a ''two-stroke charge piston'' acts in turn on the electron and hole components by means of an Auger process which occurs under restricted volume conditions and brings about a spatial separation of the charge carriers. © *2002 American Institute of Physics.*
[DOI: 10.1063/1.1511717]

1. INTRODUCTION

An unsolved mystery of porous silicon (por-Si) is the nature of its bright luminescence in the visible region of the spectrum, which is observed at room temperature and under various means of excitation. In the many papers devoted to this phenomenon a number of different factors, each of which (or in combination with others) can explain only individual properties of this luminescence. Among the main factors considered responsible for the formation of luminescence channels are the quantum size effect in the nanometer-sized silicon wires and the luminescence of the etching products on their surface. The advantages and disadvantages of these two approaches are discussed in detail not only in original papers but also in monographs (e.g., in Refs. 1 and 2). A unified explanation of the entire complex of observed properties of the emission from por-Si and of the different forms of nanostructured silicon obtained by different methods (enhanced oxidation of por-Si, the implantation of SiO_2 layers with Si^+ ions, followed by high-temperature annealing, the thermally stimulated phase separation of films of nonstoichiometric SiO_x into silicon nanoparticles and SiO_2) has not yet been achieved. Our approach to the solution of this problem is to take into account the influence of the structural inhomogeneities of the silicon nanoparticles on the formation of the luminescence properties of porous silicon.

For the majority of nanostructured silicon samples one can distinguish three levels of their structural inhomogeneity. The first level has to do with the inhomogeneity over the thickness. As is seen in Fig. 1a, even in the simplest case the samples of this material must be treated as a two-layer medium. It is obvious that the fundamental properties of the substrate material and the layer deposited on it are substantially different. A typical example of this type of object is a layer of por-Si in natural contact with monolithic silicon. In Ref. 3, in particular, it was shown that the thermal properties of por-Si layers depend on their porosity ρ; for example, at $\rho \cong 70\%$ the thermal diffusivity of por-Si layers decreases to a value equal to that of SiO_2. This means that the thermal conditions under which the por-Si layers emit depend on ρ. The difference in the degree of heating of the por-Si layers can affect, for example, the degree of thermal activation of the trap states responsible for the properties of the recombination radiation.

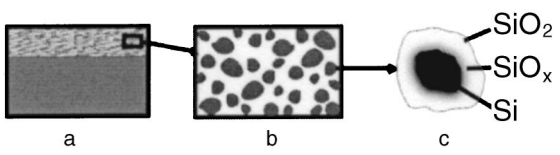

FIG. 1. Illustration of the different levels of structural inhomogeneity of porous silicon: inhomogeneity over thickness (a); variance of sizes (b); multilayer structure of individual nanocrystallites (c).

The second level of structural inhomogeneity has to do with the variance of the sizes of the silicon nanoparticles (Fig. 1b), which depends on the technological conditions. Because the band gap ΔE_g of a nanoparticle depends on its average dimension L ($\Delta E_g \propto L^{-2}$), for an ensemble of nanoparticles there is typically an inhomogeneous broadening of the electronic states, and the amount of broadening, which is thus dependent on the conditions under which the samples were prepared, is reflected in the spectral composition of the radiation, its polarization, and damping kinetics.[1,2,4–6]

Finally, the third level of the structural inhomogeneity has to do with the inhomogeneity of an individual silicon nanoparticle. As is seen in Fig. 1c, each nanocrystallite should be treated as a three-layer structure with a silicon core, a transition layer of SiO_x ($x<2$) with a gradient in terms of x, and an outer layer of SiO_2. The parameters of each of these three layers can vary over wide limits and also depend on the technology used to prepare the samples. The ensemble-averaged energy diagram of a silicon nanocrystallite with allowance for the quantum size effect, the variance of the size of the nanoparticles, the variable-gap nature of the SiO_x layer, and the numerous defect states in the SiO_x and SiO_2 layers is shown schematically in Fig. 2. The problem of determining those structural components of a multicomponent medium which are responsible for the absorption of

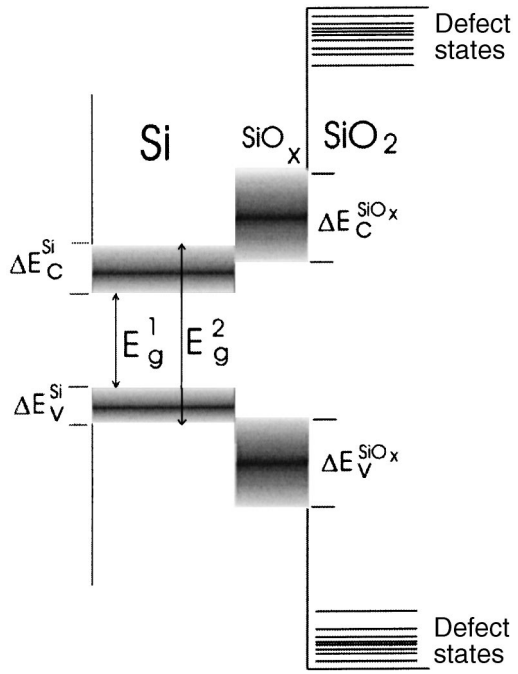

FIG. 2. Schematic diagram of the energy states of a silicon nanocrystal.

light and luminescence has to do with the third level of inhomogeneity. Very often the absorption of light occurs in one of the components and the emission in another. In that case there is also the problem of adequately describing the mechanism of transport of the charge carriers from the photoexcitation region to the secondary-emission region. Here it is important to search for signs of spatial separation of the charge carriers taking part in the radiative recombination in the multicomponent medium. In this paper we solve that problem on the basis of a comparison of the properties of the photo-, thermo-, and tunneling components of the luminescence of nanostructured silicon. A model is proposed by which the whole set of data obtained can be explained from a unified point of view.

2. EXPERIMENTAL TECHNIQUE

The basic objects of study were samples of highly oxidized por-Si and nanoparticles of silicon in SiO_2, obtained by the ion implantation. The por-Si samples were prepared by the conventional technology of electrochemical etching[1] of p-type silicon wafers having a resistivity of about $10\ \Omega$/cm and a crystallographic orientation (111) at anodizing current densities of $5-80\ \mathrm{mA/cm^2}$ and etching times of 15 to 90 min. The samples of the second type were obtained by the implantation of SiO_2 layers of the order of 500 nm thick with Si^+ ions at an irradiation dose of $6\times10^{16}\ \mathrm{cm^{-2}}$, followed by annealing for 30 min in a nitrogen atmosphere at $T_{\mathrm{ann}}=1150\,^{\circ}\mathrm{C}$.[6]

The photoluminescence (PL) was excited by radiation from a mercury lamp or a pulsed nitrogen laser with a wavelength of 337 nm. The luminescence was detected with a diffraction spectrometer with a CCD-array detector. The temperature was controlled and stabilized to 1 K or better.

The thermally stimulated luminescence (TSL) and the tunneling luminescence (TL) were measured in the temperature range 4.2–300 K on an automated device for thermally activated spectroscopic research. The TL and TSL signals were registered by a cooled photomultiplier operating in the photon-counting mode. The sample was placed in a controlled-temperature optical helium cryostat, and after cooling was irradiated by a high-pressure mercury lamp for 10–60 s at a steady temperature, which was stabilized to 0.1 K in the range 5–250 K. The kinetics of the TL were measured directly after the excitation was turned off, with a delay of 1 to 1000 s, and the signal integration time was 1 s. The technique used to measure the TL was analogous to that described previously,[7] and the details may be found in Ref. 8. The TSL was measured starting 7–15 min after excitation, when the intensity of the TL had decreased to the dark (background) signal level. The TSL was measured in two different modes: a linear heating mode, with the sample heated at a constant rate of 0.15 K/s, and a fractional thermoluminescence (FTL) mode. The fractional heating mode is a superposition of a slow linear heating of the sample and relatively low-amplitude (up to 10 K) temperature oscillations. The FTL mode, which is a modification of the initial-segment method, makes it possible to determine the activation energy for detrapping of a charge carrier to a higher accuracy and thus has a higher resolving power than the linear heating mode. This is the main advantage of using the FTL mode, since the usual methods of processing the TSL curves are extremely imprecise or altogether inapplicable in the case of a continuous or quasi-continuous distribution of the traps over energy and also when there is a discrete set of traps with very close activation energies. The details of the FTL method and the data processing are described in Refs. 9 and 10. The main difference of our implementation of the FTL method[9] from that proposed earlier[10] is the extension of the temperature interval of the measurements from liquid-nitrogen temperature down to 4.2 K, making it possible to study shallow carrier traps.

The effective average activation energy E_a is determined in each cycle of temperature oscillation by the expression

$$E_a=-\frac{d\ln I_{TSL}(T)}{d(1/k_BT)}, \tag{1}$$

where I_{TSL} is the TSL intensity, T is the temperature, and k_B is Boltzmann's constant. In accordance with the technique developed in Ref. 10, the distribution function of the filled traps $h(E)$ can be calculated to within a normalizing factor as

$$h(E)\propto\frac{I_{TSL}(E)}{dE_a/dT}, \tag{2}$$

where $I_{TSL}(E)$ is the TSL intensity after conversion of the temperature scale to an energy scale with the use of the $E_a(T)$ dependence obtained experimentally.

The TSL and TL signals, as a rule, were rather weak, ruling out the use of a monochromator for studying their spectral composition. Therefore the spectral distribution of the radiation was estimated using a set of light filters placed between the window of the cryostat and the photomultiplier.

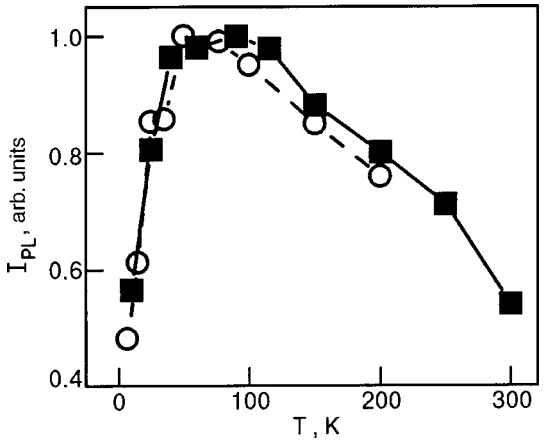

FIG. 3. Temperature dependence of the integrated PL intensity. The density of excitation is 1 kW/cm^2 (circles, dashed curve) and 20 kW/cm^2 (squares, solid curve).

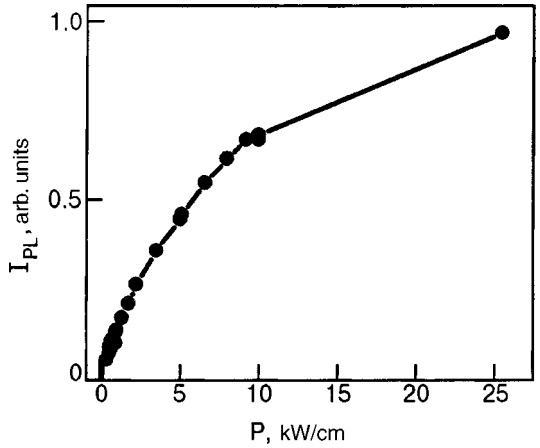

FIG. 4. Typical dependence of the integrated PL intensity of por-Si on the excitation density.

3. EXPERIMENTAL RESULTS

Photoluminescence

Let us consider those properties of the photo-, thermo-, and tunneling luminescence of nanostructured silicon that can be explained in the framework of radiation recombination of spatially separated charge carriers. Several results, in particular the temperature dependence and lux–intensity characteristic of the photoluminescence, were obtained previously in Ref. 11. Since the study of the PL of por-Si has been the subject of many papers and reviews (see, e.g. Ref. 1), we will mention only those properties of the PL which are common to samples of nanostructured silicon obtained by different technological processes. We are talking about the complex of properties of the red–orange emission band with a maximum of around 680 nm for oxidized por-Si and 740 nm for silicon nanoparticles obtained by ion implantation. We note three features of the PL of nanostructured silicon.

1. A nonmonotonic temperature dependence of the integrated photoluminescence intensity I_{PL} of the red–orange band and a dependence of the point of inversion of the sign of dI_{PL}/dT on the excitation density. As we see in Fig. 3, with increasing temperature one initially observes a growth of the integrated intensity, which gives way at high temperatures to the typical Arrhenius quenching. With increasing density of excitation the point of inversion of the sign of dI_{PL} is shifted to higher temperatures.

2. Nonlinearity of the lux–intensity characteristic of this same band, which is especially pronounced at excitation densities P above 2 kW/cm^2 (see Fig. 4).

3. Long-term degradation of the PL (the ''fatigue effect'') with an approach to a stationary value (Fig. 5). This effect displays temperature and spectral sensitivity and is most strongly expressed at the short-wavelength edge of the red–orange band at helium temperature. After the samples were heated to room temperature the emission spectrum was restored.

To explain the nonmonotonic behavior of $I_{PL}(T)$ and the dependence of the position of the point of inversion of the sign of dI_{PL}/dT on the excitation density and the technology used to prepare the samples, in Ref. 11 a model was proposed based on the assumption of a thermal detrapping of charge carriers and their subsequent localization in states from which recombination accompanied by radiation in the red–orange PL band occurs. To check this model we measured the TSL and TL of these same samples.

Thermally stimulated luminescence

TSL measurements can elucidate the role of the trap states (which are assumed to be associated structurally with the SiO_x and SiO_2 layers) in the luminescence properties of nanostructured silicon. For this it is important to study the spectral properties of the TSL. We investigated por-Si samples for which a nonmonotonic dependence of $I_{PL}(T)$ is observed. Here it should be noted that in some papers on por-Si (see the literature cited in Ref. 11) a monotonic $I_{PL}(T)$ dependence of the Arrhenius type was also observed. It was shown in Ref. 11 that the cause of that behavior is that the red–orange PL band contains a contribution from other oscillators, most likely involving residual etching products. This was confirmed by the fact that a gradual cleaning of the por-Si surface by laser ablation was accompanied by a transition from the simple Arrhenius behavior to a nonmonotonic $I_{PL}(T)$ characteristic.

Figure 6 shows typical TSL curves measured in different spectral ranges of the PL. It is known that the total PL spec-

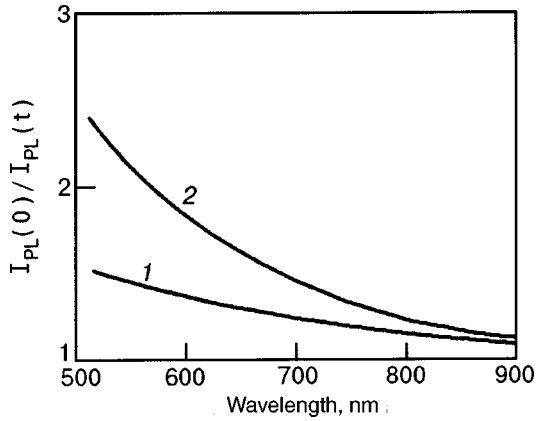

FIG. 5. Spectral dependence of the degree of degradation of the PL of por-Si at $T=6$ K, an excitation density of 30 kW/cm^2, and irradiation times t [min]: 15 (*1*) and 60 (*2*).

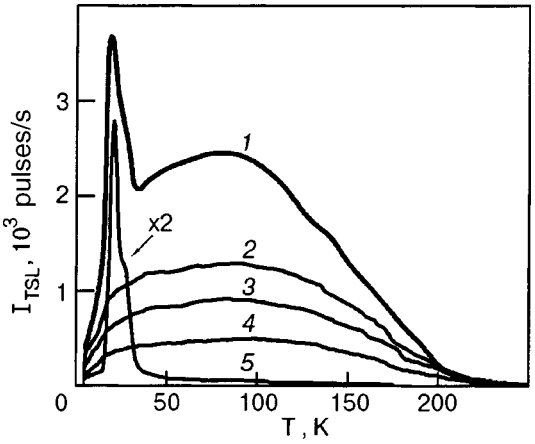

FIG. 6. Temperature dependence of the TSL signal for por-Si in different spectral ranges: total signal (detection region $\lambda > 800$ nm) (*1*), $\lambda > 640$ nm (*2*), $\lambda > 690$ nm (*3*), $\lambda > 730$ nm (*4*), $\lambda > 580$ nm (*5*).

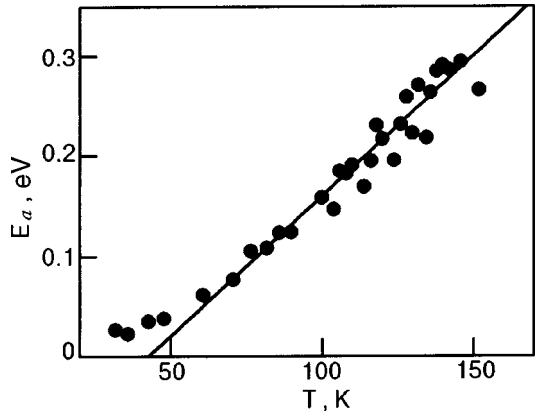

FIG. 7. Temperature dependence of the average activation energy E_a.

trum consists of a main red–orange band with a maximum at around 680 nm and a less intense blue band with a maximum at around 440 nm, the origin of which has been linked to the energy levels of defect states in the peripheral SiO_2 layer.[1] As we see in Fig. 6, the components of the emission spectrum of por-Si consist of two components of the TSL signal: a narrow low-temperature doublet near 25 K, and a wide, structureless band extending all the way to 200 K. One also notices the following features of the TSL in por-Si.

1. There is a clear correlation between the low-temperature doublet in the TSL and the blue PL band. In view of the nature of the blue PL band, the origin of the low-temperature doublet is also naturally associated with discrete trap states of a defect nature in the SiO_2 layer. This conclusion is supported by the data of Ref. 12, in which, in a study of the damping kinetics of the blue PL band in por-Si, it was observed that, in addition to the main nanosecond damping component, as the temperature is lowered from room to helium temperature, a millisecond damping component arises in a threshold manner at about 30 K, i.e., the temperature of its onset is practically equal to the position of the low-temperature component of the TSL. In Ref. 12 the appearance of the slow component of the PL kinetics is attributed to a manifestation of trap states in the emission from the peripheral SiO_2 layer. The narrowness of the low-temperature doublet in the TSL signal indicates the following features of the PL: a small variance of the energy interval between the emitting and trapping states (the blue PL band), and a narrow width of the trap level, which is more characteristic of defect states in SiO_2 than in the silicon core or the SiO_x layer, since the latter are typified by an inhomogeneous broadening of the electronic levels.

2. A comparison of the curves in Fig. 6 shows that the broad high-temperature component of the TSL signal corresponds to the red–orange PL band. Using light filters to cut out different parts of the main emission band, we found that there was no shifting or deforming of the contour of the TSL band, only a decrease in the total signal. This fact suggests that (for por-Si samples cleansed of residual etching products) the main emission band is structureless, i.e., it is not a superposition of bands of various natures.

3. The FTL technique was used to obtain the temperature dependence of the thermal activation energy E_a for the detrapping of carriers (the points in Fig. 7), which is described well by the empirical expression

$$E_a = 0.0028T - 0.12[\text{eV}]. \tag{3}$$

The energy spectrum of the trapped states responsible for the formation of the red–orange PL band can be calculated by starting from the TSL curve (curve *2* in Fig. 6) and expressions (2) and (3). It follows from the results obtained that the distribution of the traps over energy is continuous and quite wide (lying at a depth of up to 0.3 eV), its width being close to the half-width of the main PL band.

One reason why the TSL curve is so wide is the appreciable scatter of the trap states with respect to energy, apparently because of their localization in a layer of variable composition SiO_x. Another reason is the variance of the sizes of the silicon nanocrystallites, which leads to significant variation of the energy interval between the trap levels in SiO_x and the bottom of the conduction band of the silicon core (Fig. 2).

Tunneling luminescence

It is known that the detrapping of charge carriers usually occurs in a thermally activated process, but tunneling (subbarrier) transitions can also occur,[8] and they are particularly important at low temperature. The light emitted at these transitions is called tunneling luminescence. It is known that TL is an ordinary phenomenon in glasses, alkali–halide crystals, and heavily doped semiconductors,[13–15] and its damping kinetics, as a rule, obeys a Becquerel distribution law of the form $I \propto t^{-\beta}$, where t is the time and $\beta \cong 1$ is the Becquerel index. Thus the tunneling luminescence is the longest-lived emission component.

The curves of the damping kinetics of the integrated TL intensity measured in the temperature interval 5–250 K for a samples of oxidized por-Si are shown in Fig. 8. We see that the damping of the TL has a Becquerel character with an exponent $\beta \approx 1$, where β has an explicit nonmonotonic temperature dependence (Fig. 9). As far as we know, this is the first time that such a nonmonotonic $\beta(T)$ dependence has been observed in semiconductor materials.

To describe the damping kinetics of the tunneling component of the PL we consider a model based on the hopping transport of a charge carrier between localized states in the

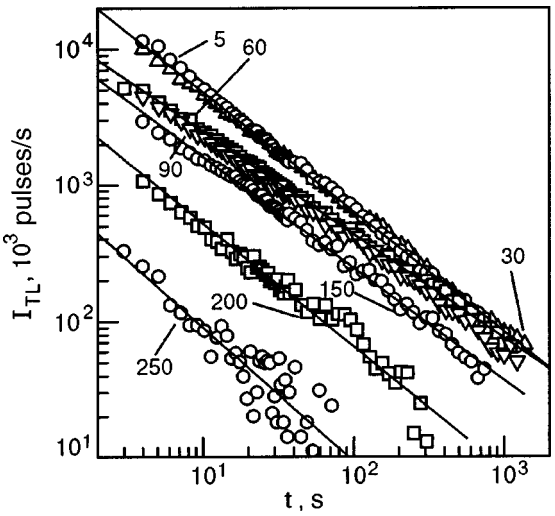

FIG. 8. Damping kinetics of the TL at different temperatures T [K], for each of which the Becquerel index β was calculated (excitation wavelength $\lambda_{exc}=405$ nm).

disordered SiO_x layer. The intensity, or the probability per unit time of a tunneling/thermally activated hop from one localized state (site) with energy ε_i to an adjacent state with energy ε_f, is described by the well-known expression[16]

$$\nu=\Gamma_{if}\exp\left(-\frac{E_{if}}{k_BT}\right), \tag{4}$$

$$\text{where}\quad E_{if}=\begin{cases}0, & \varepsilon_f\leqslant\varepsilon_i\\ \varepsilon_f-\varepsilon_i, & \varepsilon_f>\varepsilon_i\end{cases},$$

E_{if} is the activation energy of a hop, Γ_{if} is the activationless component of the hopping probability, which is determined mainly by the overlap of the wave functions of the states.

Because of the disorder in the SiO_x layer, the values of ε_i, ε_f, and Γ_{if} on going from one site to another vary in a random manner. The problem confronted by a theoretical description of the phenomenon under discussion is that the spatial distributions of these quantities and the dependence (density) of states over energy are unknown. Moreover, they can be different for different samples and even for different nanocrystallites,[1] and that also makes it difficult to do exact calculations on the basis of expression (4). Therefore, in this situation it is advisable to use the effective medium approximation (see, e.g., the review[17]). Thus we replace the spatially nonuniform quantities E_{if} and Γ_{if} in Eq. (4) by spatially uniform effective quantities E and Γ, which actually describe a process in which an electron and a hole are transported to the same site, where their recombination can occur in a single hop with a probability

$$\nu=\Gamma\exp\left(-\frac{E}{k_BT}\right), \tag{5}$$

where Γ and E are random variabes with a certain effective distribution. Such an approximation is justified in the case when the distance between the electron and hole is small (within a few hops). The admissibility of this approximation for the system under study is ensured by the small thickness of the SiO_x layer and the small size of the silicon nanocrystallite as a whole. In such an approach one can also take into account the possible transitions of the carriers from the SiO_x layer to the silicon core and back, by considering the core to be an individual trap with state energy $\varepsilon=E_g$.

Taking into account that the probability per unit time for the recombination of an electron–hole pair localized on the same site is much larger than the average hopping rate, the time dependence of the luminescence intensity I can be written as

$$I(t)=q\langle v e^{-vt}\rangle_{E,\Gamma}, \tag{6}$$

where the factor q takes into account the quantum yield of radiative recombination, and the angle brackets denote averaging over the effective distributions of Γ and E. Since we are interested in the temperature dependence of the Becquerel index, we shall replace the nearly temperature-independent quantity Γ by its average value. We then obtain the following expression for the damping kinetics of the TL:

$$I(t)=q\Gamma\int_0^\infty\exp\left[-\frac{E}{k_BT}-\Gamma t\exp\left(-\frac{E}{k_BT}\right)\right]f(E)dE. \tag{7}$$

Expression (7) can be converted to a form more convenient for analysis by taking the integral by the method of steepest descent. Such a simplification is justified for the case of the long-time asymptotic behavior that we are interested in, primarily because it is at long times that the damping has a Becquerel character. Here the saddle-point value E_0 is determined from the equation

$$k_BT\psi(E_0)=1-\Gamma t\exp\left(-\frac{E}{k_BT}\right), \tag{8}$$

$$\text{where}\quad \psi(E_0)\equiv\frac{d\ln f(E_0)}{dE_0}.$$

The physical interpretation of the method of steepest descent is rather transparent: in the course of a certain time interval from time t to $t+\Delta t$ the charge carriers that take part in emission are predominantly those which are held in traps with an activation energy close to $E_0(t,T)$. The longer the observation time t or the higher the temperature T, the larger the value of $E_0(t,T)$. For this reason, by studying the long-time asymptotics one can ''probe'' the distribution func-

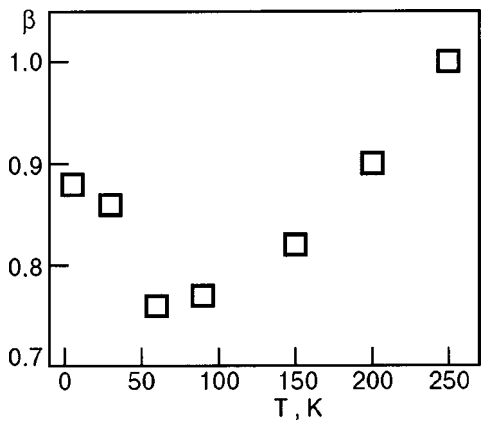

FIG. 9. Temperature dependence of the Becquerel index β.

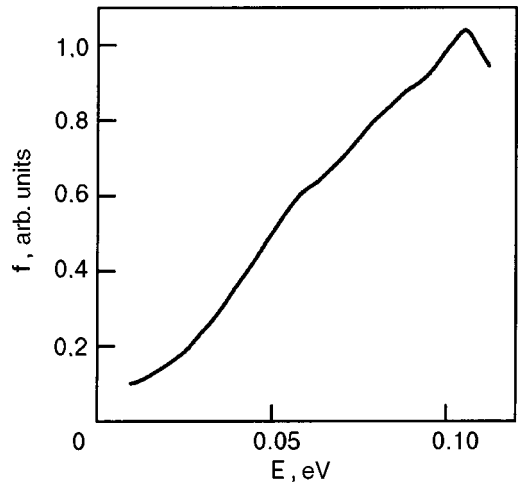

FIG. 10. Distribution function of the trapped-carrier activation energy, $f(E)$, recovered from the TL damping kinetics.

tion $f(E)$ of the effective activation energy, much as this is done by increasing T in TSL measurements. The damping exponent is given by the formula

$$\beta(t) = -\frac{d\ln I(t)}{d\ln t} = (1 - k_B T\psi) \times \left[1 - \frac{(k_B T)^2\psi' + (k_B T)^3\psi''}{2(1 - k_B T\psi - (k_B T)^2\psi')^2}\right]. \quad (9)$$

Since the TL is measured mainly at low temperature, when the condition $k_B T \ll \Delta E$ holds, where ΔE is the effective width of the distribution $f(E)$ (in practice this condition means that $\beta \approx 1$, as is observed in experiment), this allows us to make a simplification in expression (9), whereupon the relation between the Becquerel index and the energy distribution of the traps takes the simple form

$$E_0 = k_B T \ln(\Gamma t), \quad (10)$$

$$\psi(E_0) = [1 - \beta(t,T)]/k_B T. \quad (11)$$

Equation (10) establishes the relation between the energy scale, on the one hand, and the temperature and time (on a logarithmic scale) on the other. Equation (11) relates β and $\psi(E)$ [and, hence, $f(E)$, according to Eq. (8)].

From the experimental data on the TL damping kinetics (Fig. 8) we calculated the function $\psi(E)$ using expressions (10) and (11). The value $1/\Gamma \approx 0.2$ s was obtained from the condition of consistency of the kinetic curves measured at different temperatures. This value characterizes the mean time between successive activationless hops. Then, using Eq. (8), we recovered the function $f(E)$. The result of the calculation is presented in Fig. 10.

Thus the results of TSL and TL measurements are complementary and to a certain degree are in mutual agreement. The TSL gives an estimate for the width of the activation energy distribution: $\Delta E \geqslant 0.3$ eV. The TL measurements indicate a monotonic growth of the function $f(E)$ at low energies $E \leqslant 0.1$ eV. This sort of behavior can be explained by the fact that the charge carriers execute several hops prior to recombination.

4. DISCUSSION OF THE EXPERIMENTAL RESULTS

The results of the previous Section attest to the fact that a portion of the photogenerated charge carriers leave the silicon core, becoming localized in the peripheral layers of SiO_x and SiO_2. The experimental data can be explained from a unified point of view in an approach which we call the ''two-stroke charge piston'' model. It is assumed that the absorption of light with the generation of an electron–hole ($e-h$) pair occurs in the silicon core of the nanocrystallite (Fig. 11a). After this their radiative recombination can occur, with the production of a photon of secondary emission. However, the characteristic recombination time is rather long (up to several milliseconds), and therefore at the excitation densities usually used it is quite probable that prior to recombination the first $e-h$ pair will generate a second pair (Fig. 11b). As has been noted in a number of papers (see, e.g., Ref. 6), in the presence of more than two pairs of charge carriers in a nanosize silicon core a radiationless Auger recombination process becomes probable, in which the energy of recombination of one $e-h$ pair is expended on the ejection of one of the carriers of the other $e-h$ pair into the outer layer of the nanocrystallite. As a result, the nanoparticle undergoes a transition to a state in which, e.g., an electron is localized in the SiO_x layer and a hole remains in the silicon core (Fig. 11c), or vice versa. The rate of recombination of such a spatially separated $e-h$ pair is quite low because of the small probability of a tunneling transition. Therefore, when yet another $e-h$ pair is generated in a silicon core in such a state (Fig. 11d), the radiationless Auger process is again the most probable, and the result is that now a hole is ejected into the SiO_x layer (Fig. 11e). Thus the silicon core of the nanocrystallite is free of charges, which are now localized in the peripheral layers, and the core has returned to a potentially radiative state. This cyclic return of the sample to a radiative state can account for the experimentally observed ''luminescence fatigue'' effect, when the intensity of the PL does not go to zero but to a finite value of the saturation signal (Fig.

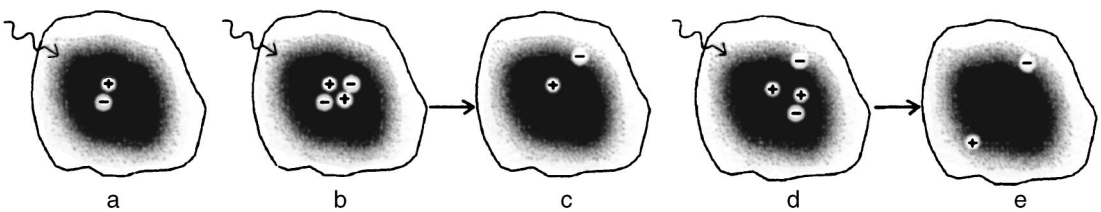

FIG. 11. Schematic illustration of the operation of the ''two-stroke charge piston'' in nanocrystalline silicon.

5). Here the efficiency of the expulsion of charge carriers in the two-cycle process described can in general be different for electrons and holes because of the difference of the energy distributions of their traps.

The model set forth above is based on the assumption of a high efficiency of the electronic Auger process, which is the motive force of the ''two-stroke charge piston,'' alternately ejecting electrons and holes from the silicon core of a nanocrystallite into its peripheral layers. This is in fact a justifiable assumption. It is known the the rate of the Auger process for free charge carriers is proportional to the square of their concentration. At a distance between interacting particles of the order of 10 nm (which corresponds to a volume density of around 10^{18} cm^{-13}) the cross section for Auger scattering is comparable to the cross section of the crystalline cell ($\sim 10^{-15}$ cm^2), i.e., it is even greater than cross section of the electron–phonon interaction.[6] Auger scattering is therefore the main dynamical process governing the lifetime of the $e-h$ pairs, the radiationless recombination time, and the other kinetic parameters of the system.

The high efficiency of the Auger process should result in efficient population of the trap states (including those of a defect nature) localized in the peripheral layers, and that circumstance is manifested in the aforementioned features of the PL spectra and of the TSL and TL signals and also their dependence on the technological conditions under which the nanostructured silicon samples were prepared. We note that the efficiency of the Auger process is higher for smaller sizes of the nanocrystallite. Therefore, the more intense TSL and TL signals are observed for samples with the smaller (on average) nanocrystallites.

Let us conclude by noting the differences between our model and that proposed in Ref. 6. The process considered in Ref. 6 ends with the transition of the nanocrystallite to a nonradiative state (corresponding to Fig. 11c), and the incomplete degradation of the PL is explained by the partly thermally activated detrapping of electrons in the peripheral layers. However, it follows from our TSL results that the majority of the trapped charge carriers are detrapped at $T > 50$ K. Therefore, to explain the quantitative degradation indices of the PL spectrum (especially near helium temperature) it is not enough to take into account only the thermal restoration of the trapped carriers: the maximum degree of degradation of the PL does not exceed a factor of three even at $T = 4.2$ K. We have therefore refined the model proposed in Ref. 6, extending the effect of the Auger process to the hole component of the electronic subsystem of the silicon core and proposing the possibility of multiple repetition of the process within a single nanocrystallite. As a result, bound charge carriers accumulate in the outer layer of the crystallite, and their recombination is manifested as features of the TSL and TL.

CONCLUSION

The luminescence properties of a system of silicon nanoparticles depends substantially on their average size and structural inhomogeneity. The influence of the size factor is manifested not only in a variation of the spectral composition of the emission due to the variation in the band gap of the nanocrystallite but also in the efficiency of the Auger process, the cross section of which is inversely proportional to the size of the crystallite. A ''two-stroke charge piston'' model is proposed, the motive force of which is the Auger process, which brings about the expulsion of charge carriers from the photoexcited silicon core of the crystallite to its peripheral oxide layers and the subsequent localization of the carriers in them. A feature of the model is the extension of the action of the Auger process successively to the electron and hole components of the silicon core. The proposed model can explain from a unified point of view a whole complex of experimental results: the nonmonotonic temperature dependence of the integrated PL intensity and the shift of the position of the extremum of this dependence on variation of the excitation density, saturation of the lux–intensity characteristic of the main PL band, the ''emission fatigue'' effect in the PL spectra, the features of the TSL signal, the presence of a tunneling component of the luminescence, and the higher intensity of TSL and TL for samples with smaller sizes of the nanocrystallites. The proposed model is of a general nature and can be invoked to explain the features of the luminescence in ensembles of nanoparticles of other semiconductors.

This study was done under the grant ''Electrical and Optical Physics of Nanostructures Based on Silicon and Germanium'' of the Russian–Ukrainian Intergovernment Program ''Nanophysics and Nanoelectronics.''

*E-mail: blon@iop.kiev.ua

[1] O. Bisi, S. Ossicini, and L. Pavesi, Surf. Sci. Rep. **38**, 1 (2000).
[2] P. Hess, *Progress in Photothermal and Photoacoustic Science and Technology*, Vol. IV Semiconductors and Electronic Materials Series, SPIE Press, Bellingham, Washington (2000).
[3] S. V. Bravina, I. V. Blonskyy, N. V. Morozovsky, and V. O. Salnikov, Ferroelectrics **254**, 65 (2001).
[4] M. S. Brodin, I. V. Blonskii, and V. A. Tkhorik, JETP Lett. **20**, 580 (1994).
[5] I. V. Blonskyy, M. S. Brodin, and V. A. Thoryk, Semicond. Sci. Technol. **12**, 11 (1997).
[6] D. Kovalev, B. Averboukh, M. Ben-Chorin, F. Koch, A. L. Efros, and M. Rosen, Phys. Rev. Lett. **77**, 2089 (1996).
[7] X. Guo and G. D. Mendenhall, Chem. Phys. Lett. **152**, 146 (1988).
[8] A. Kadashchuk, Yu. Skryshevskii, A. Vakhnin, N. Ostapenko, V. I. Arkhipov, E. V. Emelianova, and H. Bässler, Phys. Rev. B **63**, 115205 (2001).
[9] A. Kadashchuk, D. S. Weiss, P. M. Borsenberger, S. Nespurek, N. Ostapenko, and V. Zaika, Chem. Phys. **247**, 307 (1999).
[10] I. A. Tale, Phys. Status Solidi A **66**, 65 (1981).
[11] S. N. Bashchenko, I. V. Blonskiĭ, M. S. Brodyn, V. N. Kadan, and Yu. A. Skryshevskiĭ, Zh. Tekh. Fiz. **71**(1), 66 (2001) [Tech. Phys. **46**, 63 (2001)].
[12] A. Kux, D. Kovalev, and F. Koch, Appl. Phys. Lett. **66**, 49 (1995).
[13] D. E. Aboltin, V. J. Grabovskis, A. R. Kangro, Ch. Lushchik, A. A. O'Konnel-Bronin, I. K. Vitol, and V. E. Zizap, Phys. Status Solidi A **47**, 667 (1978).
[14] E. A. Kotomin and A. B. Doktorov, Phys. Status Solidi B **114**, 287 (1982).
[15] K. G. Zamaraev, R. F. Zaĭrutdinov, and V. P. Zhdanov, *Electron Tunneling in Chemistry: Chemical Reactions at Large Distances* [in Russian], Nauka, Novosibirsk (1985).
[16] A. Miller and E. Abrahams, Phys. Rev. **120**, 745 (1960).
[17] J. W. Haus and K. W. Kehr, Phys. Rep. **150**, 263 (1987).

Translated by Steve Torstveit